

RESEARCH

Design and Analysis of Meander Coil Electromagnetic Acoustic Transducer (EMAT) for Multi-mode Lamb Waves in Thin Plate

R. Dhayalan* 

Nondestructive Evaluation
Division, Indira Gandhi
Centre for Atomic
Research,
Kalpakkam 603102, India

***Corresponding author:**

E-mail:
dhayalanr@gmail.com
dhayalanr@igcar.gov.in

ABSTRACT

The generation and detection of multi-mode Lamb or plate waves in thin aluminum plate materials using Meander coil electromagnetic acoustic transducers (EMAT) is presented in this paper. EMAT works under the Lorentz force principle in non-magnetic materials. The generation of lower order or fundamental Lamb waves (S_0 and A_0) has been performed in both finite element (FE) simulations and experimental measurements. This paper is divided into three parts; first 2-D electromagnetic simulation model has been created for the Lorentz force calculation which is coupled by the induced or eddy current inside the material and the applied static magnetic field. The Lorentz force causes the vibration of sound waves inside the aluminum material. Second, the calculated Lorentz force densities are utilized as input sources for the generation of transient ultrasonic waves within the aluminum material. Third, the multimode Lamb waves (S_0 and A_0) have been excited with two different coil spacing EMATs and compared with experimental measurements. The interaction of multimode Lamb waves with an artificially created notch has also been analyzed and compared for both experiments and FE simulations. It has been observed that the simulation results agreed very well with the experimental measurements.

KEYWORDS

Meander coil EMAT, finite element modeling, Lorentz force density, multi-mode Lamb waves, and dispersion curves.

INTRODUCTION

Electromagnetic Acoustic Transducers (EMATs) are advanced, non-contact, electromagnetic based ultrasonic transducers now widely being used for non-destructive evaluation (NDE) applications [1-3]. This type of transducer generally consists of high-frequency RF coils and magnets to excite as well as receive ultrasonic sound waves using the Lorentz force principle in non-magnetic materials like aluminum, stainless steel, etc., It can also generate and receive sound waves using magnetostriction or in combination with Lorentz force mechanism in ferromagnetic materials like mild steel, carbon steel, etc., [4-6]. EMATs have a lot of advantages the conventional piezoelectric-based and other type's ultrasonic transducers. EMATs don't require liquid couplant (non-contact) which eliminates the inconsistency in measurements during the testing. The cleaning of the material surface is not required

while using the EMAT since the wave generation originates within the material. EMAT can also be used for high temperature measurements whereas the other type of ultrasonic transducers have their limitations. EMAT can able to generate all types of sound wave modes including shear horizontal waves which are quite difficult to generate by conventional transducers. The different types of ultrasonic wave generation depend upon the coil geometry and the application of the magnetic field. It is possible to excite and receive ultrasonic guided waves or Lamb waves or plate waves in thin metallic materials simply by changing the coil geometry and/or the direction of the magnetic field. Customized EMATs can be easily fabricated and quite compatible than other transducers. A brief discussion about the basic principle of EMAT, the various NDE applications, and the advantage of EMAT are explained in more detail elsewhere [6-9].

Lamb (guided) waves are known as plate waves which are commonly used for the testing of metallic materials and structures. It is mainly used for structural health and condition monitoring applications. These waves can be generated and propagated in thin materials in which the thickness is smaller or equivalent to the wavelength. The generation and propagation of Lamb waves depend on the material properties and thickness of the material [10-11]. When compared to ultrasonic bulk waves, Lamb waves propagate through the entire thickness of the material and can test the complete volume of the material with a single or two measurements. It is widely used in various NDE applications, such as metal plate testing, composites testing, adhesive bond testing, and reactor vessel inspection [12-14]. Generally, the Lamb waves are divided into two categories; symmetric (S) or dilatational and asymmetric (A) or bending wave modes [10,11]. The lower order or the fundamental Lamb wave modes (S0 and A0) can be generated at low frequencies. Considerable research works have been carried out on the development of various types of EMAT for exciting Lamb waves metallic materials [15-17]. All the EMATs were designed with different coil designs including spiral coil, linear coil, elongated spiral coil, and Meander coil. These coil designs were mainly focused to generate a single Lamb wave mode at low frequencies. The generation of single Lamb wave mode with different types EMATs were studied numerically and experimentally and these EMATs were mainly used for long-range ultrasonic testing. In this paper, the finite element (FE) analysis of Meander coil EMAT with two different coil spacing is presented for generating the multimode (S0 and A0) Lamb waves on a thin aluminum plate. The Meander coil EMATs with the same design features are developed for experimental measurements. Then, the interaction of multimode Lamb waves with artificial, slot-type defect and the comparison of FE simulation results with measurements are also presented in this paper.

This paper is divided into four parts; first, a two-dimensional (2D) FE electromagnetic model is designed for the Lorentz force density on a thin aluminum material. Second, the force densities are utilized as the input sources for generating the multimode Lamb waves on the aluminum material. Third, a set of Meander coil EMATs with two different coil spacings have been developed to generate multimode Lamb waves on a thin aluminum plate for experimental studies. Finally, the interaction of multimode Lamb waves with an artificial notch has been carried out and the results obtained from both the simulations and measurements have been analyzed and compared with each other.

ELECTROMAGNETIC MODEL FOR MEANDER COIL EMAT

To calculate the Lorentz force densities for the Meander coil EMAT, a 2D electromagnetic model (EM) is created with a high-frequency RF coil, a permanent magnet, and a

non-magnetic ($\mu_r = \mu_0$) test material. For the transmission mode, the RF coil is used to excite with a high alternating current (AC) pulse, and the permanent magnet is used to induce a strong static magnetic flux on the test material. The AC pulse flows on the EMAT coil induce image or eddy currents (j_e) inside the test material and in the presence of a strong magnetic flux (B_s); the induced eddy currents interact with the bias magnetic field and create the Lorentz force distribution (F_L) inside the test material. In general, the maximum force generation occurs within one wavelength depth from the surface of the test material and it is also called the electromagnetic skin depth [1-3],

$$\vec{F}_L = \vec{j}_e \times \vec{B}_s \quad (1)$$

The Lorentz forces (F_L) generated inside the test material are transmitted through collisions within the lattice level. Further, it causes vibrations of sound waves at the same frequency as the AC pulse used for exciting the EMAT coil. Thus the Lorentz force densities generate ultrasonic waves in the non-magnetic test material. The type of ultrasonic wave and its physical features mainly depend upon the coil design and the application of the magnetic field [6-8]. Fig 1(a) shows the schematic of an EMAT with only one current-carrying coil and a normal biasing permanent magnet leading the generation of Lorentz force inside the test material.

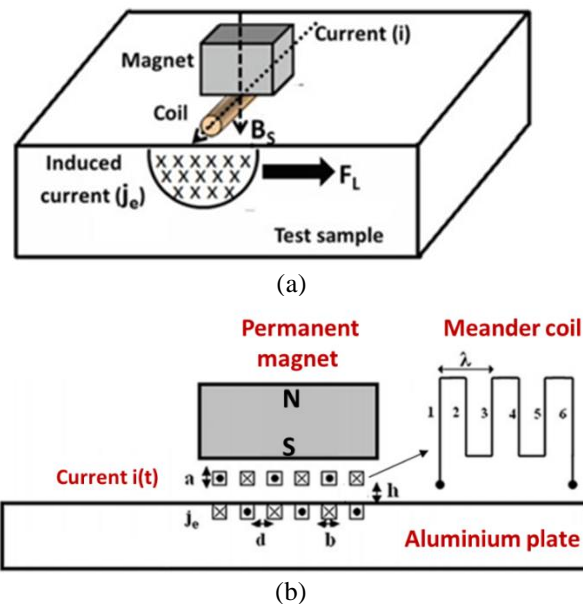


Fig. 1. (a) Schematic of an EMAT with one coil and a permanent magnet generates the Lorentz force inside the test material and (b) EM model showing the arrangement of the Meander coil, permanent magnet, and aluminum plate.

The 2D FE simulation for the EM has been performed by using the commercial finite element software COMSOL. It has predefined modules with in-built mathematical formulations to facilitate EM modeling. Fig 1(b) shows the EM model of the Meander coil EMAT with the arrangement of the coil, permanent magnet, and a 2 mm

thickness aluminum plate. The sintered Neodymium-Iron-Boron (NdFeB) magnet with a flux density of 0.35 T is used for the permanent magnet. Copper is chosen as the material for the excitation coil (electrical conductivity of 5.9×10^7 S/m and density of 8700 kg/m^3) and six turns are used for two different coil spacings. The dimension of the coil is 0.75 mm in length and 0.5 mm in thickness. The transient input current fed to the Meander coil for excitation is assumed to be given by [18],

$$i_k(t) = \beta e^{-\alpha(t-\tau)^2} \cos(2\pi f_c(t - \tau) + \phi) \quad (2)$$

where, β is the maximum amplitude of input current i.e., 50 Ampere, α is the bandwidth factor which determines the number of cycles in the excitation pulse here it is set to be $5 \times 10^{11} \text{ sec}^{-2}$, τ is the half-width of the excitation pulse (3×10^{-6} s), ϕ is the phase difference and f_c is the central frequency of the input excitation pulse i.e., 500 kHz. The distance between the coil and the material surface i.e., coil lift-off is 1 mm. Fig. 2(a) shows the input AC pulse with 6 μ s time duration used for exciting the Meander coil at 500 kHz central frequency. This input current is fed to the Meander coil which is shown in Fig. 1(b). When a time-varying input current is passed through the Meander coil kept above an aluminum plate, image or eddy current induced inside the material [4,5]. In the presence of an external magnetic field, eddy current interact with the field and generates Lorentz force distribution within the material. From equation (1), the force densities are directly calculated by multiplying the static magnetic field and the eddy current density. Fig. 2(b) shows the calculated Lorentz force densities underneath of the coil 1 and coil 2 from the right side of the Meander coil which is kept near to the top surface of the material. It has been observed that the time history of the Lorentz force follows the same as the input excitation current and this observation has been done at central frequency of 500 kHz.

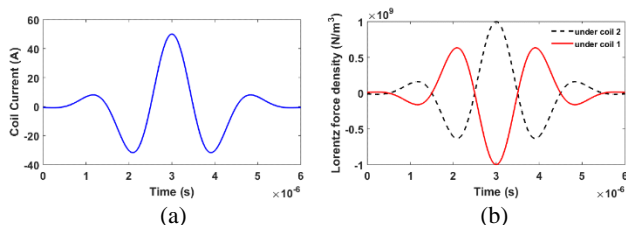


Fig. 2. (a) The input AC pulse for exciting the Meander coil at 500 kHz and (b) the calculated Lorentz force densities on the top surface of the aluminum plate.

ULTRASONIC WAVE PROPAGATION MODEL

The FE modeling of Meander coil EMAT for ultrasonic wave propagation has been performed by using ABAQUS explicit method. The wave propagation model is created by using the structural mechanics module to solve the transient dynamic and quasi-static analyses [19]. The Lorentz force values calculated from the EM model are applied as inputs for generating ultrasonic waves in the wave propagation

model. The simulation of ultrasonic wave propagation for Meander coil EMAT can also be performed by using COMSOL, however, the implicit solver takes a larger computation time and not converging for a bulk structure at high frequencies. The transient time increment (Δt) and the element size (L) are very small which in turn result in unstable, oscillatory solution and fail to converge. In general, the stability condition of a FE model is always based on the smallest time increment of the wave propagates across any of the element sizes which can also express as,

$$\Delta t \approx \frac{L}{C} \quad (3)$$

where, L is the smallest mesh size and C is the wave velocity inside the material. In this paper, a 2D plane strain model is created by using ABAQUS explicit scheme for generating ultrasonic Lamb waves in a thin aluminum plate. The physical and mechanical properties of aluminum are imposed for the discrete model and the computed force values are utilized as inputs for the wave propagation simulation. The calculated force densities are applied as concentrated forces on the thin aluminum plate. When the forces inputs are applied, ultrasonic Lamb waves have been generated within the aluminum plate. The generation of time-dependent elastic waves can be written in terms of the force, displacement, and density of the material as

$$\mu \nabla \times \nabla \times \vec{u} - (\lambda + 2\mu) \nabla \nabla \cdot \vec{u} + \rho \frac{\partial^2 \vec{u}}{\partial t^2} = \vec{f}_L \quad (4)$$

In equation (4), ρ is the density of the material and u is the displacement vector. The details of FE simulation parameters used for wave propagation modeling are provided in Table 1.

Table 1. The Abaqus simulation parameters used for wave propagation.

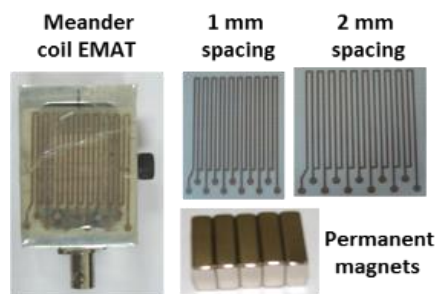
Material	Aluminum
Density (ρ)	2700 kg/m ³
Young's modulus (E)	70 Gpa
Poisson's ratio (ν)	0.3
Longitudinal velocity (C_L)	6320 m/s
Shear velocity (C_S)	3140 m/s
Frequency (f_c)	500 kHz
Mesh size (L)	0.0003 m
Mesh type	4-noded bilinear quadrilateral element
Time increment (Δt)	1e-8 s
Lame constant (μ)	2.76e-10 N/m ²
Lame constant (λ)	5.19e-10 N/m ²

Though the Meander coil EMAT excitation region is very small compared to the entire aluminum plate which is spatially discretized into discrete element sizes in the order of 1/15th of the elastic wavelength. Since the FE model is created in 2D plane strain condition, a 4-noded bilinear quadrilateral element with reduced integration (CPE4R) is considered for meshing the aluminum plate. The reduced integration decreases the formation of elements during meshing and the computation time for the whole model.

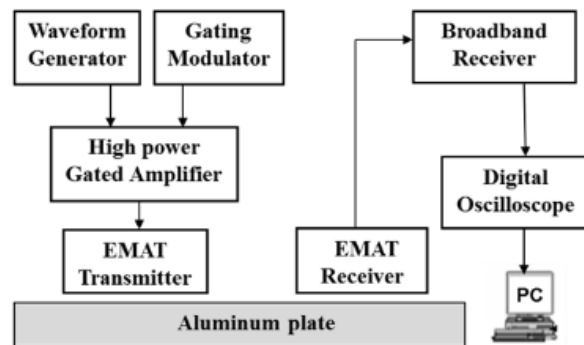
The dynamic FE model uses an algorithm for computing the displacements of time-dependent elastic stress generated within the aluminum plate. The incremental time or the time step has been optimized based on the stability condition given in Equation (3). There are two steps have been assumed for wave propagation, namely the excitation step and propagation step. The force inputs are applied to the aluminum plate during the excitation step. In the next propagation step, the multimode Lamb waves generated by the Meander coil EMAT are allowed to propagate inside the aluminum plate.

EXPERIMENTAL DETAILS

In general, the Meander coil EMATs are usually developed with copper coils and normal biasing electromagnets or permanent magnets. As mentioned earlier, the generation of ultrasonic wave modes and excitation frequency depends upon the coil design, dimensions, and the applied magnetic field. The Meander coils should be enough flexible to bend and twist for curved surfaces, hence it is made by using the flexible printed circuit board (PCB) method. This method provides any arbitrary coil design with very high accuracy in dimensions. The PCB Meander coils are made from 150 μm thickness polyester-based laminates with copper cladding of 50 μm thickness. Two coil spacing i.e. 1 mm and 2 mm spacing are used to develop the Meander coil EMATs. Sintered NdFeB permanent magnets of dimensions 25 x 25 x 15 mm are utilized to develop the Meander coil EMATs. The magnets exhibit a flux density of around 0.35 T at the end faces. **Fig. 3(a)** shows the developed Meander coil EMAT with two different coil spacings and permanent magnets. The Meander coil EMAT generates periodic driving shear traction forces inside the aluminum material when the coil is excited with a time-varying current with a normal biasing magnetic field. Because of the alternating coil spacing, the direction of the force densities changes alternatively concerning the excitation plane on the material. The alternating force density causes the vibration of sound waves inside the material. It generates the Rayleigh or surface waves that propagate along the surface of the material [18]. It also generates the angle beam shear and longitudinal waves simultaneously inside the material. The Meander coil EMAT generates all these bulk wave modes in thick materials where the thickness is higher than the wavelength. Because of the coil symmetry, it generates these waves in bi-directional mode in the material i.e., it generates from both sides of the EMAT transmitter. Depending upon the coil spacing, frequency, and plate thickness, the Meander coil EMAT generates the Lamb or plate wave modes in thin aluminum plates. It generates Lamb waves in thin plates where the thickness is equivalent to or less than the wavelength (coil spacing) [20,21]. **Fig. 3(b)** shows the schematic of the measurement set-up used for generating the multimode Lamb waves on the thin aluminum plate using Meander coil EMATs.



(a)



(b)

Fig. 3. (a) Meander coil EMAT designed with flexible coils (PCB), and permanent NdFeB magnets, and. (b) Schematic diagram for the experimental measurements.

In order to validate the FE simulation results, the Meander coil EMATs have been developed for the experimental measurements. The details of various parameters used for the measurements are provided in **Table 2**.

Table 2. The details of experimental parameters used for measurements.

1	Excitation current	50 Ampere
2	Input Voltage	1 Vpp
3	Coil lift -off	1 mm
4	Magnetic flux density	0.35 T
5	Central frequency	500 kHz
6	Receiver gain	42 dB
7	Time averaging	16 times
8	Low pass filter	3 MHz
9	High pass filter	50 kHz
10	Digitization rate	50 MS/s

A 50-ampere sinusoidal tone burst signal of 500 kHz is used for exciting the transmitter EMAT coil. This input signal is obtained from a high-power gated amplifier connected with an arbitrary waveform or function generator and a gating modulator. The function generator continuously generates a sine wave signal with 1 Vpp amplitude which is fed to the high-power gated amplifier. The gating modulator determines the number of cycles, pulse duration, and pulse repetition rate for the input signal. A low noise, broadband receiver amplifier is used to increase the signal strength with 42 dB gain settings for the

receiver side EMAT. The received signals are monitored and acquired with the aid of a digital oscilloscope interfaced with a personal computer.

Results obtained with Meander coil EMATs

Generation and detection of multimode Lamb waves

The Meander coil EMAT with two different coil spacings has been designed and analyzed in both experiments and FE simulations. The EMATs designed with 1 mm and 2 mm coil spacings are utilized to generate the multimode Lamb waves on a 2 mm thickness aluminum plate. A set of two aluminum plates of the same size (750x400x2 mm) are used for this work in which the first one is a defect-free plate to analyze the Meander coil EMAT with two different coil spacings. In the second sample, an electro-discharge

machining (EDM) notch of size (20x0.5x0.5 mm) is made to check the defect detection capability of EMAT. Through-transmission or pitch-catch (separate transmitter and receiver) technique is used for both measurements. To analyze the Meander coil EMAT with two different coil spacings, the transmitter EMAT is excited to generate the multimode Lamb waves on the defect-free aluminum plate, and the same are captured by another, essentially identical, receiver EMAT. The transmitter EMAT is kept at a distance of 100 mm away from the receiver EMAT which is positioned along the acoustic axis to receive the generated Lamb wave modes. **Fig. 4** shows the schematic of the measurement set up for the generation and detection of multimode Lamb waves on the defect-free aluminum plate at 500 kHz.

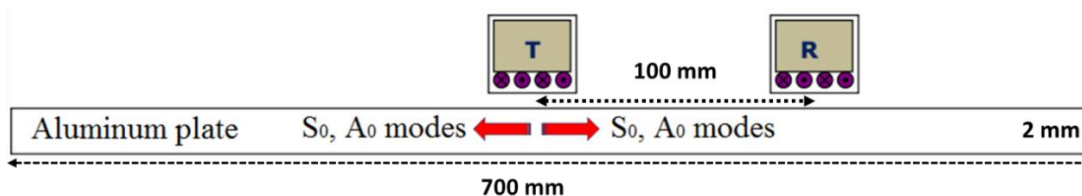


Fig. 4. Schematic of the measurement setup used for the generation and detection of multimode Lamb waves using Meander coil EMAT.

The phase velocity and group velocity dispersion curves for a 2 mm thickness aluminum plate are plotted by using Disperse software and are shown in **Fig. 5(a)** and **Fig. 5(b)** respectively. From these curves, it can be seen that the Meander coil EMAT generates the lower order or fundamental (S0 and A0) modes at 500 kHz [22]. The Lamb wave modes (S0 and A0) are fairly non-dispersive at this frequency and their group velocities are 5324 m/s and 3313 m/s respectively.

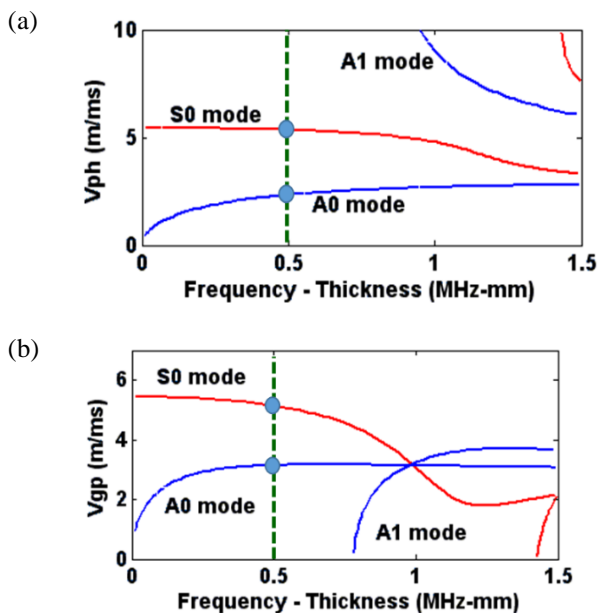


Fig. 5. (a) Phase velocity and (b) group velocity dispersion curves for 2 mm thickness aluminium plate.

The designed Meander coil EMATs with 1 mm and 2 mm coil spacing are utilized to generate the fundamental S0 and A0 modes on the defect-free aluminum plate. **Figs. 6(a)** and **6(b)** show the time domain A-scan signals of multimode Lamb wave obtained at 500 kHz from the experimental measurements and FE simulations.

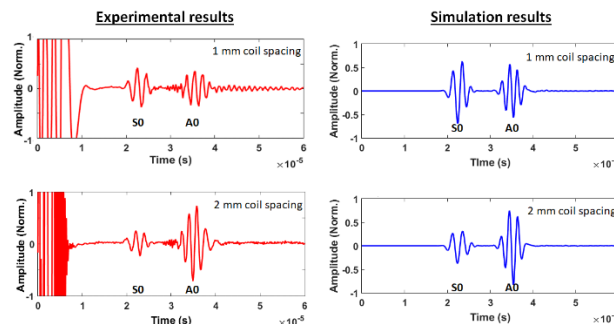


Fig. 6. Comparison of time histories of the A-scan signals obtained with two different Meander coil spacings from the (a) experiments and (b) FE simulations.

From the experimental and FE simulation results, the first arrived signals are the S0 modes and the later signals are the A0 modes. The calculated group velocity for the S0 mode is ~5320 m/s and for the A0 mode is ~3310 m/s. It has been observed that the signal amplitudes are higher for the wider (2 mm) coil spacing when compared to closer (1 mm) coil spacing. This is mainly attributed that the force densities are more for the wider spacing coil than the closer spacing coil. It has also been noticed that the generated wave modes are fairly non dispersive for both coil spacings. From **Fig. (6)**, the FE simulation results are line with the experimental measurements in all the aspects.

Defect detection with multimode Lamb waves

In order to check the detection capability, the Meander coil EMAT designed with 2 mm coil spacing has been used on the defective aluminum sample. The multimode Lamb waves are generated and allowed to propagate through the EDM notch with 0.5 mm depth. The schematic diagram for the measurement set-up is shown in Fig. 7. When the multimode Lamb waves interact with the notch defect, each mode gets the mode converted into its own and the other existing mode at the same frequency. This mode conversion happens for each mode while reflection and transmission through the defect. This is mainly due to the sudden

variation in plate thickness. Fig. 8 compares the FE simulation and experimental outputs of multimode Lamb waves interacting with a 0.5 mm depth defect.

From both the FE simulation and experimental outputs, the time of arrival, mode shape, and signal amplitudes of the mode converted and reflected Lamb wave signals are fairly in good agreement with each other. When the incident S₀ mode interacts with the notch, it gets mode converted into S₀ and A₀ modes in both reflection and transmission through the notch. This is also valid for the incident A₀ mode. The mode converted and scattered S₀ and A₀ are identified and analyzed from the time of flights and the distances traveled by each wave modes.

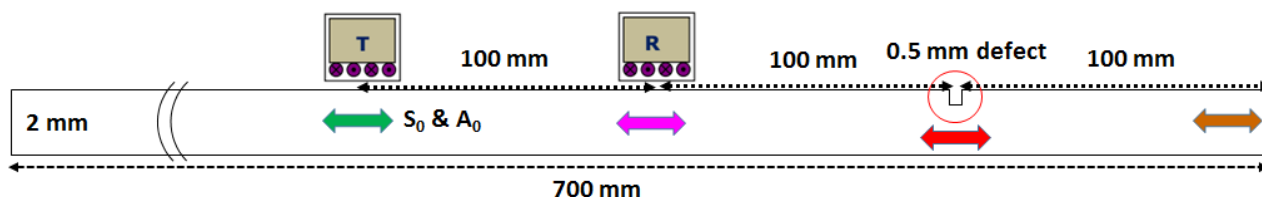


Fig. 7. Measurement setup for defect detection using multimode Lamb waves.

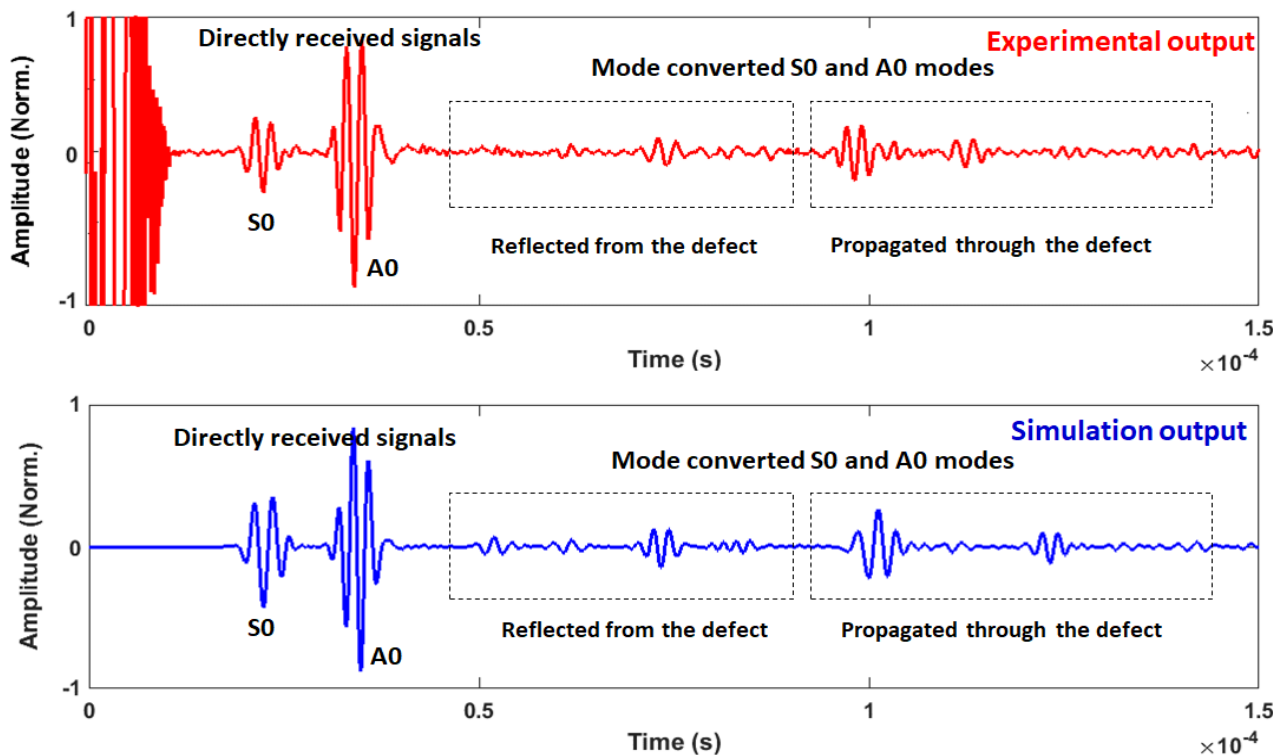


Fig. 8. Defect detection using multimode Lamb wave modes and comparison of FE simulation and experimental outputs.

CONCLUSION

A complete FE modeling system is designed for Meander coil EMAT works under the Lorentz force principle on non-ferromagnetic (aluminum) material. First, an EM model is designed with copper coils and a normal biasing magnet for the force density calculations within the material. Second,

the wave propagation model is designed in which the dynamic forces are utilized as sources for radiating ultrasonic Lamb waves inside the aluminum material. To validate the FE simulation results, Meander coil EMATs have been developed with two different coil spacings using flexible PCB coils and sintered NdFeB permanent magnets for the experimental measurements. The multimode or

fundamental (S0 and A0) Lamb waves have been generated at 500 kHz and analyzed for two different coil spacings. The time histories of multimode Lamb waves obtained from the experimental measurements are compared with FE simulation results. The interaction of multimode Lamb waves with an artificial notch defect has been performed and the results obtained with experiments and FE simulations are analyzed and compared with each other. It has been observed that the fundamental S0 and A0 Lamb wave modes get the mode converted into its own and the other existing mode at the same excitation frequency. It has been noticed that the mode conversion happens for each mode while reflection and transmission through the defect. The mode converted and the scattered Lamb wave modes are identified and analyzed from the time of arrival and the distances traveled by the individual wave modes. It has also been observed that the FE simulation outputs are matching very well with the experimental measurements.

ACKNOWLEDGEMENTS

This work is a part of the author's final year M. Tech project at the Department of Physics, NIT Tiruchirappalli. The author would like to acknowledge Prof. Krishnan Balasubramaniam (External guide), Department of Mechanical Engineering, IIT Madras, for allowing carrying out his final year M. Tech at the Centre for Nondestructive Evaluation (CNDE). The author would also like to acknowledge Prof. A.R. Ganesan (Internal guide), Department of Physics, IIT Madras.

REFERENCES

- Maxfield, B.W.; Fortunko, C.M.; Mater. Eval., **1983**, 41, 1399-1408.
- Hirao, M.; Ogi, H.; EMATs for science and industry- non-contacting ultrasonic measurements; Kluwer Academic Publishers, Boston, **2003**.
- Jian, X.; Dixon, S.; Edwards, S.R.; Non-Dest. Eval., **2005**, 20 42- 62.
- Thompson, R. B.; Physical principles of measurements with EMAT transducers, in: Physical Acoustics, Thurston, R.N.; Pierce, A.D.; (Eds.); 19 San Diego: Academic Press, New York, **1990**, 157-200.
- Dhayalan, R.; Satyanarayanmurthy, V.; Krishnamurthy, C.V.; Balasubramaniam, K.; *Ultrasonics*, **2011**, 51, 675-682.
- Maxfield, B.W.; Kuramoto, A.; Hulbert, J.K.; *Mater. Eval.*, **1987**, 45(10), 1166-1183.
- Arun, K.; Dhayalan, R.; Balasubramaniam, K.; Maxfield, B.W.; Patrick, P.; Barnoncel, D.; An EMAT based shear horizontal wave (SH) technique for adhesive bond inspection, Review of Progress in Quantitative Nondestructive Evaluation (QNDE 2012), AIP conf. Proc. Vol. 1430, 1268-1275, **2012**.
- Silk, M.G.; (Ed.); Electromagnetic Acoustic Transducers, Ultrasonic Transducers for Nondestructive Testing, Adam Hilger Ltd, Bristol, UK, **1984**.
- Ludwig, V.B.; Werner, R.; Schmid, R.; Friedrich, M.; Kroning, K.; *Nucl. Engg. Design*, **1994**, 151, 539-550.
- Rose, J.L.; *Ultrasonic Waves in Solid Media*, Cambridge University Press, UK, **1999**.
- Luo, W.; Rose, J.L.; *Insight*, **2003**, 45, 1-5.
- Alleyne, D.N.; Cawley, P.; *NDT & E Inter.*, **1992**, 25, 11-22.
- Masserey, B.; Raemy, C., Fromme, P.; *Ultrasonics*, **2014**, 54(7), 1720-1728.
- Dhayalan, R.; Rajkumar, K.V.; Anish Kumar, Mukhopadhyay, C.K.; *Ann. of Nucl. Ener.*, **2019**, 133, 795-804.
- Xie, Y.; Liu, Z.; Yin, L.; Wu, J.; Deng, P.; Yin, W.; *Ultrasonics*, **2017**, 73, 262-270.
- Ratnam, D.; Balasubramaniam, K.; Maxfield, B.W.; *IEEE Trans. Ultrason. Ferroelectr. Freq. Control.*, **2012**, 59(4), 727-737.
- Sun, W.; Liu, G.; Xia, H.; Xia, Z.; *Sensors and Actu. A Phys.*, **2018**, 282, 251-258.
- Dhayalan, R.; Balasubramaniam, K.; *Nondest. Testing and Eval.*, **2010**, 26, 101-118.
- ABAQUS Inc. Analysis user's manual, section 22.2.3—2D solid element library, version 6.6-1. Palo Alto, CA: ABAQUS, Inc., **2006**.
- Murayama, R.; Mizutani, K.; *Ultrasonics*, **2002**, 40, 491-495.
- Dhayalan, R.; Balasubramaniam, K.; *NDT & E Inter.*, **2010**, 43, 519-526.
- Lowe, M.; Pavlakovic, B.; *DISPERSE user's manual and introduction*, version 2.0.16B (NDTL), Imperial College, London, **2003**.



This article is licensed under a Creative Commons Attribution 4.0 International License, which allows for use, sharing, adaptation, distribution, and reproduction in any medium or format, as long as appropriate credit is given to the original author(s) and the source, a link to the Creative Commons license is provided, and changes are indicated. Unless otherwise indicated in a credit line to the materials, the images or other third-party materials in this article are included in the article's Creative Commons license. If the materials are not covered by the Creative Commons license and your intended use is not permitted by statutory regulation or exceeds the permitted use, you must seek permission from the copyright holder directly.

Visit <http://creativecommons.org/licenses/by/4.0/> to view a copy of this license.